Supporting Information

Conditions for the Efficiency of Optical Limiting Based on Experiment and Quantum Chemical Calculations

Alexander Yu. Tolbin, [a*] Mikhail S. Savelyev, [b,c] Pavel N. Vasilevsky, [b] and Alexander Yu. Gerasimenko[b,d]

[a] FSBIS Institute of Physiologically Active Compounds of the Russian Academy of Sciences, Russian Academy of Sciences, 142432, Chernogolovka, Severny proezd, 1, Moscow Region, Russian Federation
[b] National Research University of Electronic Technology Institute of Biomedical Systems, 124498, Zelenograd, Moscow, Russian Federation
[c] Laboratory of Clinical Smart Nanotechnologies, Institute for Regenerative Medicine, Sechenov University, 119991, Moscow, Bolshaya Pirogovskaya st., 2, Russian Federation.
[d] Institute for Bionic Technologies and Engineering, Sechenov University, 119991, Moscow, Bolshaya Pirogovskaya st., 2, Russian Federation.

[*] Corresponding author. Tel.: +7 496 5242566, e-mail address: tolbin@ipac.ac.ru (Prof. A.Yu. Tolbin), ORCID 0000-0002-5541-5401.

TABLE OF CONTENTS

1. DFT Calculations

Quantum chemical calculations were performed using density functional theory (DFT) implemented with exchange-correlation functional M06 [1] and aug-cc-pVDZ basis set.[2]

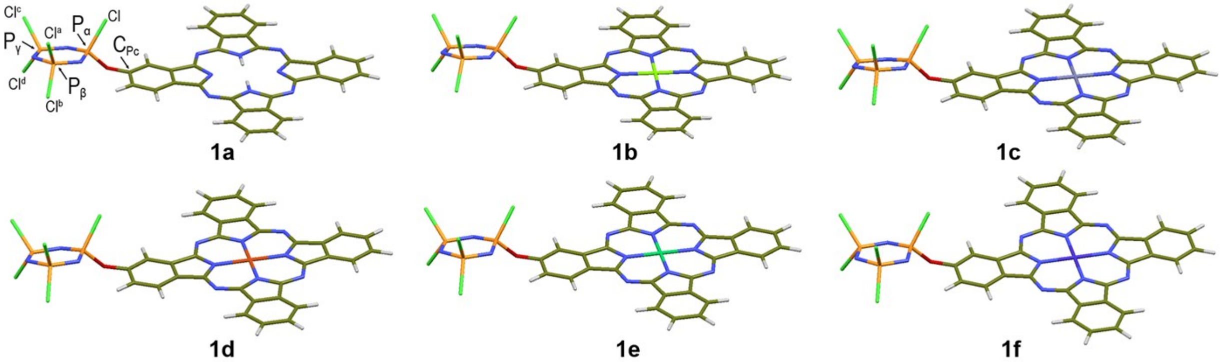

1a 1b 1c

1d 1e 1f

Figure S1. DFT-optimized structures of model dyes **1a–f** (M06/aug–cc–pVDZ).

The calculated parameters are shown in Table S1.

Table S1. Geometric parameters of structures of dye models **1a–f** according to the DFT methods (M06/aug–cc–pVDZ).

Property	**Structure**					
	1a	**1b**	**1c**	**1d**	**1e**	**1f**
Multiplicity	Singlet	Singlet	Singlet	Doublet	Singlet	Doublet
Bond length P_α–Cl, Å	2.059	2.058	2.058	2.058	2.058	2.058
Valence angle Cl–P_α–O, deg.	103.0	102.9	102.9	102.9	102.9	102.9
Valence angle P_α–O–C_{Pc}, deg.	124.4	124.2	124.0	124.3	124.5	124.3
Bond length P_β–Cl^a, Å	2.052	2.052	2.052	2.052	2.052	2.052
Bond length P_β–Cl^b, Å	2.052	2.052	2.053	2.052	2.052	2.052
Valence angle Cl^a– P_β–Cl^b, deg.	101.0	101.0	101.0	101.0	101.0	101.0
Bond length P_γ–Cl^c, Å	2.051	2.050	2.050	2.050	2.050	2.050
Bond length P_γ–Cl^d, Å	2.049	2.049	2.049	2.049	2.049	2.049
Valence angle Cl^c– P_γ–Cl^d, deg.	101.2	101.2	101.2	101.2	101.2	101.2
Angle between phosphazene and phthalocyanine planes, deg.	13.3	15.7	19.6	15.2	12.5	15.6

The angles between bonds of the characteristic atoms P, O, Cl, and C_{Pc} as well as the lengths of the P–Cl bonds are almost the same for all structures. Hence, the chemical properties of compounds **1a–f** concerning the peripheral modification should not differ significantly.

Under the influence of a field, as its strength increases, the P–Cl bond lengths become greater, and this is most noticeable for P_β–Cl_a and P_γ–Cl_c, i.e. for chlorine atoms in *trans*-position to the phthalocyanine ring compared to the analogous P_β–Cl_b and P_γ–Cl_d bonds, where the chlorine atoms are in the *cis-* configuration (Table S2). The length of the P_α–Cl bond remains virtually unchanged, which may indicate its chemical stability during an attempt to form a bimacrocyclic molecule in which the macrocycles are in the *ipso*-configuration. In our previous work, we showed the impossibility of the existence of such a structure, [3] and here we find another confirmation of this fact. At the same time, the bond angles Cl–P–Cl, Cl–P–O, and P–O–C remain almost unchanged.

Table S2. Geometric parameters of the structures of dye models **1a–f**, optimized in the presence of an electric field F=(–0.006;0;0.006), according to the FF–DFT methods (M06/aug–cc–pVDZ). For the excited molecules, the index "†" is used.

Property	**Structure**					
	3a†	**3b†**	**3c†**	**3d†**	**3e†**	**3f†**
Multiplicity	Singlet	Singlet	Singlet	Doublet	Singlet	Doublet
Bond length P_{α}–Cl, Å	2.077	2.079	2.078	2.085	2.077	2.084
Valence angle Cl–P_{α}–O, deg.	103.0	102.7	103.6	101.4	103.6	101.4
Valence angle P_{α}–O–C_{Pc}, deg.	129.3	129.4	127.2	128.3	127.1	128.3
Bond length P_{β}–Cl^{a}, Å	2.278	2.308	2.251	2.410	2.245	2.409
Bond length P_{β}–Cl^{b}, Å	2.194	2.211	2.204	2.296	2.199	2.299
Valence angle Cl^{a}– P_{β}–Cl^{b}, deg.	106.2	108.1	104.5	121.4	104.2	121.3
Bond length P_{γ}–Cl^{c}, Å	2.146	2.142	2.145	2.127	2.146	2.127
Bond length P_{γ}–Cl^{d}, Å	2.108	2.106	2.116	2.099	2.117	2.099
Valence angle Cl^{c}– P_{γ}–Cl^{d}, deg.	99.5	99.2	99.8	97.9	99.9	97.9
Angle between phosphazene and phthalocyanine planes, deg.	10.9	12.0	6.4	4.7	5.7	4.3

2. Laser experiments

2.1. Analytical expressions

The solution to the radiative transfer equation (RTE) [4] for the general dependence of the absorption coefficient η on the intensity I is written by the expression:

$$\int_{I_0(\rho,\varphi,t)}^{I(\rho,\varphi,t)} \frac{1}{I\eta(I)} dI = -d, \qquad (S1)$$

where I_0 is the incident intensity, ρ and φ – are the polar coordinates, t – is time, and d – is the optical path length.

During the experiment, the values of the total pulse energy U are determined to calculate the transmission values T. Intensity I in the general case is determined by the total pulse energy by the formula:

$$I = UA(\rho)B(\varphi)C(t), \qquad (S2)$$

in which $A(\rho)$ is the radial pulse profile; ρ – is the distance from the axis of the laser beam; $B(\varphi)$ – is the angular dependence of the pulse profile; φ – is the angular coordinate, and $C(t)$ – is the shape of the pulse over time t.

Commonly, to process the experimental results on the interaction of laser radiation with a nonlinear medium, which consists of approximating the relationship between normalized transmission and intensity, the postulate is used that laser pulses have a Gaussian shape, and this makes it possible to implement many theories.[5, 6] However, obtaining a solution in elementary functions is not always possible. At the same time, it was noted that the NLO response weakly depends on the pulse shape and is determined mainly by the energy parameters of the laser. Therefore, in calculations it is advisable to use expressions for the rectangular pulse shape, for which an analytical solution can almost always be obtained:

$$\begin{cases} A(\rho) = \left(w^2\pi\right)^{-1} \; (0 \le \rho \le w) \\ B(\varphi) = 1 \; (0 \le \varphi \le 2\pi) \\ C(t) = 1/\tau \; (0 \le t \le \tau) \end{cases} \qquad (S3)$$

The values of nonlinear transmission (the ratio of the transmitted and incident pulses) are normalized to linear transmission (it is determined by the linear absorption coefficient α). After including the threshold intensity $I_\times$ in the expression for the absorption coefficient $\eta(I)$ as follows:

$$\eta(I) = \alpha + \beta\left(I - I_\times\right) \cdot H\left[I - I_\times\right], \qquad (S4)$$

and substituting this equation into Eqn. S1, considering the general expression for the intensity (Eqn. S2) and the nature of the pulse intensity distribution (Eqn. S3), we obtain a formula for determining the normalized transmission T_N from the solution of the RTE in the following view:

$$T_N = \exp\left(-\frac{\beta}{\tau}\left(\frac{U}{w(z)^2\pi} - I_\times\right) \cdot d\right) \qquad (S5)$$

In this expression: $w(z)$ – is the beam radius depending on the distance to the lens focus z: $w(z) = w_0\sqrt{1 + z^2/z_0^2}$, where w_0 – is the beam radius at the lens focus; $z_0 = \pi w_0^2/\lambda$ – is the Rayleigh length related to the wavelength λ. Formula S4 includes the Heaviside function **H**, which is responsible for turning on an additional term for the nonlinear absorption coefficient β or turning it off, leaving only the linear absorption coefficient α.

2.3. Measurement results

Below are the output signals of optical limiters based on dyes **1a-f** and z-scan curves demonstrating nonlinear pattern of absorption of intense laser radiation. The multiparametric Eqn. S5 allows determining not only the nonlinear absorption coefficient β, but also the limiting threshold $I_\times$.

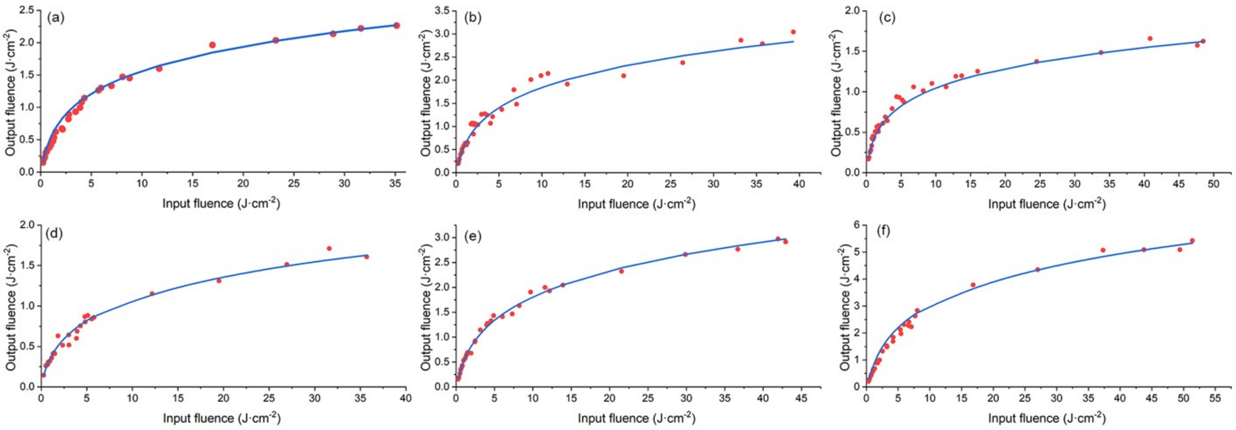

Figure S2. Optical limiting output signals of phthalocyanines **1a-f**: laser Nd:YAG – see Fig. 2 in the main text; pulse duration – 16 ns; wavelength – 532 nm; optical pathlength – 0.2 cm.

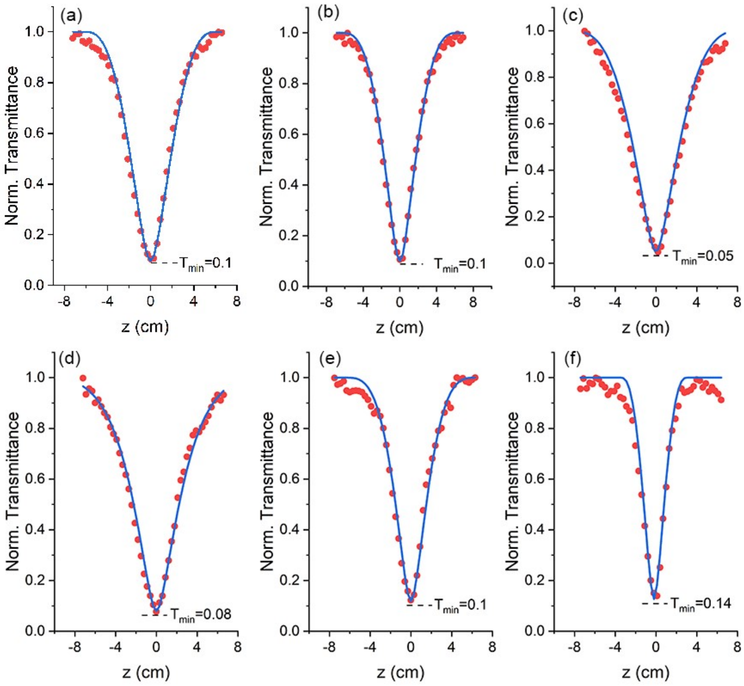

Figure S3. Z-Scan curves (open aperture) to determine nonlinear absorption coefficient β and limiting threshold $I_{\times}$ for phthalocyanines **1a-f**: laser Nd:YAG – see Fig. 2 in the main text; pulse duration – 16 ns; wavelength – 532 nm; optical pathlength – 0.2 cm.

3. Analytical expressions

Solving inequalities 8–11 (see main text) in Wolfram Mathematica 10.0 gives the following solution for α:

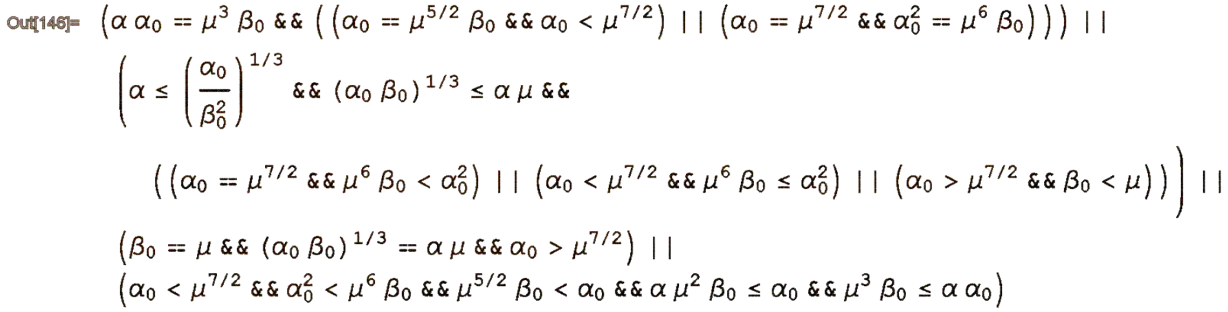

Out[146]=

$$\left(\alpha\,\alpha_0 == \mu^3\,\beta_0 \;\&\&\; \left(\left(\alpha_0 == \mu^{5/2}\,\beta_0 \;\&\&\; \alpha_0 < \mu^{7/2}\right) \;||\; \left(\alpha_0 == \mu^{7/2} \;\&\&\; \alpha_0^2 == \mu^6\,\beta_0\right)\right)\right) \;||$$

$$\left(\alpha \le \left(\frac{\alpha_0}{\beta_0^2}\right)^{1/3} \;\&\&\; (\alpha_0\,\beta_0)^{1/3} \le \alpha\,\mu \;\&\& \right.$$

$$\left.\left(\left(\alpha_0 == \mu^{7/2} \;\&\&\; \mu^6\,\beta_0 < \alpha_0^2\right) \;||\; \left(\alpha_0 < \mu^{7/2} \;\&\&\; \mu^6\,\beta_0 \le \alpha_0^2\right) \;||\; \left(\alpha_0 > \mu^{7/2} \;\&\&\; \beta_0 < \mu\right)\right)\right) \;||$$

$$\left(\beta_0 == \mu \;\&\&\; (\alpha_0\,\beta_0)^{1/3} == \alpha\,\mu \;\&\&\; \alpha_0 > \mu^{7/2}\right) \;||$$

$$\left(\alpha_0 < \mu^{7/2} \;\&\&\; \alpha_0^2 < \mu^6\,\beta_0 \;\&\&\; \mu^{5/2}\,\beta_0 < \alpha_0 \;\&\&\; \alpha\,\mu^2\,\beta_0 \le \alpha_0 \;\&\&\; \mu^3\,\beta_0 \le \alpha\,\alpha_0\right)$$

4. References

1. Y. Zhao and D. G. Truhlar, *Theoretical Chemistry Accounts*, 2008, **120**, 215-241.
2. T. H. Dunning, *The Journal of Chemical Physics*, 1989, **90**, 1007-1023.
3. A. Y. Tolbin, B. N. Tarasevich, M. K. Beklemishev, V. K. Brel and V. E. Pushkarev, *ChemistrySelect*, 2022, **7**, e202201065.
4. M. S. Savelyev, A. Y. Gerasimenko, V. M. Podgaetskii, S. A. Tereshchenko, S. V. Selishchev and A. Y. Tolbin, *Optics & Laser Technology*, 2019, **117**, 272-279.
5. O. Muller, V. Pichot, L. Merlat and D. Spitzer, *Scientific Reports*, 2019, **9**, 519.
6. A. A. Said, M. Sheik-Bahae, D. J. Hagan, T. H. Wei, J. Wang, J. Young and E. W. Van Stryland, *J. Opt. Soc. Am. B*, 1992, **9**, 405-414.